Available online at www.sciencedirect.com
SCIENCE DIRECT®
Catalysis Today 89 (2004) 465–478
CATALYSIS TODAY
www.elsevier.com/locate/cattod

# Development of sulfur tolerant catalysts for the synthesis of high quality transportation fuels

Naoto Koizumi, Kazuhito Murai, Toshihiko Ozaki, Muneyoshi Yamada*

*Department of Applied Chemistry, Graduate School of Engineering, Tohoku University, Aoba 07, Aramaki, Aoba-ku, Sendai 980-8579, Japan*

Received 17 September 2003; received in revised form 16 December 2003; accepted 2 February 2004

Available online 24 April 2004

**Abstract**

In this paper, results concerning the development of sulfur tolerant catalysts for Fischer–Tropsch synthesis (FTS), $C_{2+}$ alcohol synthesis, methanol and/or DME synthesis are presented. In the FTS reaction on Fe using $H_2$-rich syngas such as the biomass-derived syngas, the composition of catalyst pretreatment gas and the addition of MnO on Fe had strong impacts on its sulfur resistance as well as activity. Especially the Fe/MnO catalyst pretreated with CO showed a much lower deactivation rate and a higher FTS activity than an Fe/Cu/K catalyst in the presence of $H_2S$. For $C_{2+}$ alcohol synthesis a novel preparation method was developed for a highly active $MoS_2$-based catalyst that is well known as the sulfur tolerant catalyst. Besides some metal sulfides were found to show higher CO hydrogenation activities than $MoS_2$. In particular, both Rh and Pd sulfides were active and selective for the methanol synthesis. Modified Pd sulfide catalyst, i.e. sulfided Ca/Pd/$SiO_2$, showed an activity that was about 60% of that of a Cu/ZnO/$Al_2O_3$ catalyst in the absence of $H_2S$. This catalyst preserved 35% of the initial activity even in the presence of $H_2S$. The sulfided Ca/Pd/$SiO_2$ mixed with γ-$Al_2O_3$ was also available for in situ DME synthesis in the presence of $H_2S$.


*Keywords:* Sulfur tolerant catalysts; Fischer–Tropsch synthesis; Methanol synthesis; DME synthesis; Fe-based catalysts; Transition metal sulfide catalysts

## 1. Introduction

It has been generally assumed that catalysts for CO hydrogenation such as Fischer–Tropsch synthesis (FTS) and methanol synthesis are poisoned by a small amount of sulfur compounds in the feed [1,2]. For example, a Cu/ZnO/$Al_2O_3$ catalyst loses its methanol synthesis activity even in the presence of $H_2S$ 1.6 ppm in concentration [2]. Sulfur content in the syngas is, however, seriously high especially when the syngas is produced from a coal and heavy oil. The syngas produced from biomass and waste materials that are thought to be promising carbon resources in future contains $H_2S$ to some extent also. Berg et al. [3], for example, reported that $H_2S$ content is in a range from 20 to 200 ppm when the syngas is produced from a non-catalytic gasification of biomass while the syngas from waste plastics contains $H_2S$ and COS 300 ppm in concentration [4]. To avoid the sulfur poisoning, conventional plants are equipped with a huge desulfurizer unit that removes the sulfur compounds almost completely from the feed (usually below 1 ppm).

Considering these situations, the development of sulfur tolerant catalysts is expected to contribute for increasing a versatility of the syn-fuel process. For example, the use of the sulfur tolerant catalyst can simplify the conventional, huge and complex process by omitting the desulfurizer unit, which is quite advantageous for developing a novel on-site process that produces transportation fuels in the vicinity of small-scale and dispersed carbon resources. Besides, various carbon resources such as remote gas fields, biomass and waste materials as well as various process conditions for their reforming process, e.g. steam reforming, non-catalytic partial oxidation or gasification, become available.

So far, several attempts were made to improve the sulfur tolerance of the CO hydrogenation catalysts. Attentions were mainly focused on the reaction using the coal-derived syngas that have low $H_2$/CO ratios and contain large amounts of $H_2S$ ($10^3$ to $10^4$ ppm). For the FTS reaction using the CO-rich

* Corresponding author. Tel.: +81-22-217-7214; fax: +81-22-217-7293.
*E-mail address:* yamada@erec.che.tohoku.ac.jp (M. Yamada).

0920-5861/$ – see front matter © 2004 Elsevier B.V. All rights reserved.
doi:10.1016/j.cattod.2004.02.002

syngas Fe-based catalysts are more suitable than Co-based catalysts because of their water–gas shift activity. Moreover, Davis and his coworkers [5] have recently reported that the FTS activity of Fe catalysts is comparable or higher than that of Co catalysts when they are compared at temperatures that produce low levels of $CH_4$ and at relatively high space velocities. In 1960s, Anderson and coworkers [6–9] investigated the sulfur poisoning of the Fe-based catalysts and effects of the activation method and the additive on the deactivation rate of the catalysts using the CO-rich syngas. They found that nitrided and CO-pretreated catalysts show lower deactivation rates in the presence of the gaseous $H_2S$ than $H_2$-pretreated catalyst [8]. Later the addition of large amounts of Mn oxide (MnO) is found to improve the sulfur resistance much more effectively in both the FTS reactions using the CO-rich and the $H_2$-rich syngas [10]. The deactivation rate of this catalyst is about one hundredth of that of an Fe/Cu/K catalyst in the presence of $H_2S$ 300 ppm in concentration. It should be noted that the addition of large amounts of MnO strongly affects the selectivity of the Fe catalyst as well. The precipitated Fe/MnO shows a higher selectivity for $C_2$–$C_4$ olefins (or $C_2$–$C_3$ hydrocarbon) than the precipitated Fe catalyst [11,12], suggesting that MnO modifies the nature of the active site over the precipitated Fe catalyst.

In contrast to these conventional metallic catalysts, an alkaline metal-promoted Mo sulfide catalyst preserves its initial activity for the synthesis of mixed alcohols for a long period even in the presence of $H_2S$ 50 ppm in concentration [13,14]. In other words Mo sulfide-based catalysts have an excellent sulfur tolerance. The performance of the Mo sulfide-based catalysts is, however, not adequate since this catalyst requires higher reaction pressures (usually above 10 MPa) to attain activities and selectivities for $C_{2+}$ alcohol synthesis comparable with those of Cu-based catalysts. It is also worthy to note here that CO hydrogenation activities of transition metal sulfides except for Mo and W sulfides have not been investigated yet.

In this paper, recent attempts to develop the sulfur tolerant catalysts for the synthesis of the transportation fuels are presented. Attentions have been paid to develop the sulfur tolerant catalysts that show higher activities for the synthesis of $C_{10}$–$C_{20}$ hydrocarbon, $C_{2+}$ alcohol, dimethyl ether (DME) and/or methanol because both $C_{10}$–$C_{20}$ hydrocarbon and DME are most promising substituted diesel fuels. Besides, $C_{2+}$ alcohol is useful for the gasoline additive and methanol (and/or DME) is the fuel for the fuel cell. Considering the previous results mentioned above, effects of the catalyst activation method and the MnO addition on both the FTS activity and the sulfur resistance of the Fe catalyst have been investigated when the $H_2$-rich syngas is used as the feed. This is important because the syngas produced from the non-catalytic gasification of biomass is rich in $H_2$. The authors have also tried to make clear the reason in relation with the surface fine structure of the catalyst why the MnO addition greatly improves the sulfur resistance of the Fe catalyst. Then, a novel preparation method has been developed for a highly active $MoS_2$-based catalyst for $C_{2+}$ alcohol synthesis whereas $MoS_2$ has been reported to be prepared by the thermal decomposition or the reduction of $(NH_4)_2MoS_4$ (ATTM) in the previous studies on the mixed alcohols synthesis. Besides, the CO hydrogenation activities and selectivities of various transition metal sulfides have been investigated to find novel catalysts that show higher activities for this reaction.

## 2. Improvements in the activity and the sulfur resistance of the Fe FTS catalyst

### 2.1. Effect of the activation method

Syngas is usually produced by a steam reforming or partial oxidation of carbon resources such as coal, natural gas and biomass. The syngas derived from the coal is rich in CO and has the $H_2$/CO molar ratio from 0.5 to 1.0 whereas the syngas derived from biomass is rich in $H_2$ ($H_2$/CO molar ratio: 2–3). Because Fe catalysts have water–gas shift activities they are more suitable for the FTS reaction using the CO-rich syngas than Co and Ru catalysts. Before the reaction the Fe catalysts are usually pretreated for the activation in a stream of $H_2$, CO or the syngas. Many studies showed that the FTS activity of the catalysts depend on the composition of the pretreatment gas. A CO-pretreated catalyst shows a higher activity than a $H_2$ or syngas-pretreated one. It is considered that Fe carbide ($Fe_xC$) is an active species [15,16], and that the CO pretreatment is effective for the formation of $Fe_xC$ [17–20]. Besides the CO-pretreated catalyst shows a superior sulfur resistance than the $H_2$-pretreated one [9], although the reason why the CO pretreatment is effective for improving the sulfur resistance is not clear.

Recently, attentions have been paid to the utilization of the biomass-derived syngas from the “carbon neutral” point of view. Since Fe is low-cost compared with Co and/or Ru, the Fe catalyst is more suitable for the conversion of the biomass-derived syngas. Moreover, Davis and coworkers [5] have recently reported that the FTS activity of Fe catalysts is comparable or higher than that of Co catalysts when they are compared at temperatures that produce low levels of $CH_4$ and at relatively high space velocities. As concerns the composition of the feed gas, it has been already reported that the Fe catalyst pretreated with CO shows a higher CO conversion whereas the chain growth probability of the formed hydrocarbon is lower when using the $H_2$-rich syngas as the feed instead of the CO-rich syngas [21]. However, effects of the composition of the pretreatment gas on the activity and the sulfur resistance of the Fe catalysts in the FTS reaction using the $H_2$-rich syngas have never been investigated yet. Thus these issues have been investigated, especially in relation with the formation of the Fe carbide.

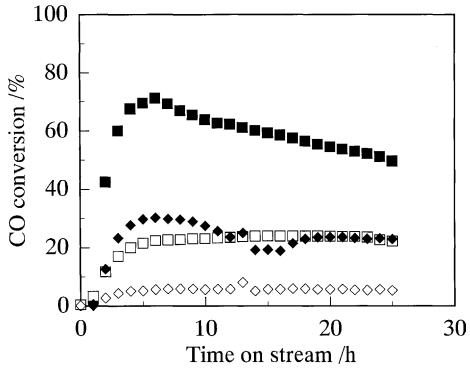


Fig. 1. Effects of the catalyst pretreatment procedures on the CO conversion over the Fe catalyst: (■) CO-pretreated sample (feed gas: $H_2/CO = 2.0$), (□) $H_2$-pretreated sample (feed gas: $H_2/CO = 2.0$), (◆) CO-pretreated sample (feed gas: $H_2/CO = 0.67$), (◇) $H_2$-pretreated sample (feed gas: $H_2/CO = 0.7$). Reaction conditions: 503 K, 1.6 MPa.

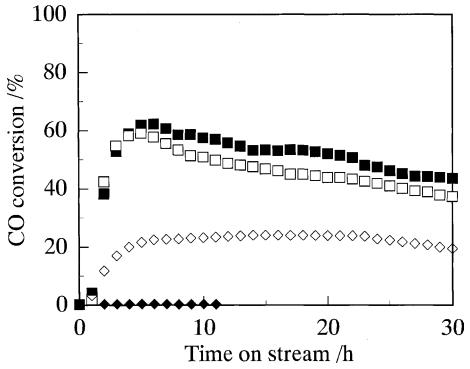


Fig. 2. Catalytic properties of the Fe catalysts pretreated with various gases from the $H_2$ rich syngas: (□) CO-pretreated sample, (■) CO then $H_2S$-treated sample, (◇) $H_2$-pretreated sample, (◆) $H_2$ then $H_2S$ treated sample. Reaction conditions: 503 K, 1.6 MPa.

### 2.1.1. FTS activity

A precipitated Fe catalyst was pretreated in a stream of $H_2$ or CO and then subjected to the FTS reaction at 503 K and 1.6 MPa using a $H_2$-rich syngas ($H_2/CO$ molar ratio: 2). Fig. 1 shows CO conversions as a function of the time on-stream. This figure also shows a conversion when the FTS reactions are performed using a CO-rich syngas ($H_2/CO$ molar ratio: 0.67) for comparison. As already reported by Davis and coworkers [22], the Fe catalyst pretreated with CO shows a higher CO conversion than the catalyst pretreated with $H_2$ for the reaction using the CO-rich syngas. In consistent with the previous result, the CO-pretreated Fe catalyst shows a higher CO conversion for the reaction using the $H_2$-rich syngas. It is also revealed in the present study that the chain growth probability of the hydrocarbon over the CO-pretreated catalyst is slightly lower than that over the $H_2$-pretreated catalyst while the CO-pretreated catalyst is less selective for the $CO_2$ formation than the $H_2$-pretreated one when the $H_2$-rich syngas is used as the feed.

To make clear the structure-activity relationship for the Fe FTS catalyst, powder XRD and BET surface area measurements were performed. Powder XRD measurements of the catalysts before the FTS reaction indicated the formation of α-Fe and χ-$Fe_{2.5}$ C over the $H_2$-pretreated catalyst and the CO-pretreated catalyst, respectively. BET surface area of the $H_2$-pretreated catalyst was much smaller than that of the CO-pretreated one. After the FTS reaction using the $H_2$-rich syngas, the Fe carbides (χ-$Fe_{2.5}$ C and ε′-$Fe_{2.2}$C) were formed over the $H_2$-pretreated catalyst whereas $Fe_2O_3$ was detected as well as χ-$Fe_{2.5}$ C over the CO-pretreated one. Considering the results reported in the literature [23], we suggest that the decline in CO conversion on the CO-pretreated catalyst is caused by the transformation of the carbide phase to $Fe_3O_4$. It was also found that the heating rate during the CO pretreatment has a strong impact upon the formation of χ-$Fe_{2.5}$ C, and that the catalysts show higher FTS activities when the formation of χ-$Fe_{2.5}$ C is promoted. From these results it is suggested that the Fe carbide ($Fe_xC$) is also active species for the FTS reaction using the $H_2$-rich syngas. The lower CO conversion of the $H_2$-pretreated catalyst can be responsible for the quite lower BET surface area of the catalyst.

### 2.1.2. Sulfur resistance

Then the effect of the carbide formation upon the sulfur resistance of the Fe catalyst has been investigated. For this purpose the $H_2$ or CO-pretreated catalyst was further treated with 1000 ppm $H_2S$/He at 373 K in situ. $H_2S$ treated catalysts were then subjected to the FTS reaction in the absence of $H_2S$. In Fig. 2 CO conversions over variously treated catalysts are shown as a function of the time on-stream. The catalyst treated with CO then $H_2S$ shows a CO conversion comparable with that over the CO-pretreated one. The chain growth probability of the hydrocarbon over the catalyst treated with CO then $H_2S$ was slightly lower than that over the CO-pretreated catalyst (0.75 versus 0.78). On the other hand the catalyst treated with $H_2$ then $H_2S$ shows no activity at all. Thus the CO pretreated catalyst shows a superior sulfur resistance than the $H_2$-pretreated one.

The $H_2S$ treatment subsequent to the $H_2$ or CO pretreatment had little influence on the BET surface area and the powder XRD pattern of the catalyst. On the other hand XPS measurements showed that only the peak assigned to FeS appears in the spectrum of the catalyst treated with $H_2$ then $H_2S$ whereas the peaks assigned to FeS and $Fe_xC$ appear in the spectrum of the catalyst treated with CO then $H_2S$. These results suggest that the reason why the CO-pretreated catalyst shows the superior sulfur resistance is that the Fe carbide is more difficult to be sulfided during the subsequent $H_2S$ treatment than α-Fe.

## 2.2. Effect of the MnO addition

The addition of MnO on Fe has a strong impact on its FTS activity and selectivity. The Fe/MnO catalyst shows a higher selectivity for $C_2$–$C_4$ olefin than the Fe catalyst [11,12]. Since $C_2$–$C_4$ olefin is useful for the chemical

feedstock, effects of the Fe/Mn ratio [11,12], the activation method and the reaction conditions [24] were investigated. Apart from these studies Chaffee et al. [10] found that the Fe/MnO catalyst shows a superior sulfur resistance than the Fe/Cu/K catalyst in both the FTS reactions using the $H_2$-rich and/or the CO-rich syngas. Most of previous works dealing with this type of catalyst, however, focused on its activity for the light alkene synthesis. Thus the effects of the Fe/Mn ratio and the activation method on the $C_{10}$–$C_{20}$ hydrocarbon synthesis activity and the sulfur resistance of the Fe/MnO catalyst are not yet so clear. Besides the effect of the MnO addition on the surface fine structure (not bulk structure) and the adsorption property of the surface species over the Fe catalyst has never been investigated. To develop the FTS catalyst that shows a superior sulfur resistance, the effects of the Fe/Mn ratio and the activation method on the $C_{10}$–$C_{20}$ hydrocarbon synthesis activity and the sulfur resistance of the Fe/MnO catalyst have been investigated at first. Then the surface fine structure and the adsorption property of the surface species over the Fe/MnO catalyst have been examined by means of diffuse reflectance IR Fourier transform (DRIFT) spectroscopy using CO as a surface probe molecule to make clear the reason why the MnO addition improves the sulfur resistance of the Fe catalyst.

### 2.2.1. Hydrocarbon synthesis activity and sulfur resistance [25]

Fe/MnO catalysts with various Fe/Mn atomic ratios were prepared by the precipitation method and then were pretreated in the stream of a syngas (33% CO/62% $H_2$/5% Ar). The FTS reaction was carried out at 523 K and 1.6 MPa using the same syngas as a feed. The formation rate of hydrocarbon over the Fe/MnO catalyst normalized to the total Fe atoms increased with increasing the Fe/Mn atomic ratio whereas the chain growth probability of the formed hydrocarbon decreased. The formation rate and the chain growth probability of the hydrocarbon formed over the catalyst with the Fe/Mn ratio of 0.17 (Fe/MnO (1/6)) were lower than those over an Fe/Cu/K catalyst.

Fig. 3 shows formation rates of the hydrocarbon over the Fe/MnO (1/6) catalyst pretreated with $H_2$, CO or CO/$H_2$ normalized to the total Fe atoms. This figure also shows chain growth probabilities of the formed hydrocarbon. From this figure the Fe/MnO (1/6) catalyst pretreated with CO shows the highest formation rate of the hydrocarbon. The chain growth probability of the hydrocarbon formed over this catalyst is also highest. Both these values are comparable with those over the Fe/Cu/K catalyst.

Then the effect of the composition of the pretreatment gas on a sulfur resistance of the Fe/MnO (1/6) catalyst was further investigated. After the FTS activity of the catalyst reached its steady state under the sulfur-free conditions, the syngas mixed with 0.1% $H_2S/H_2$ was fed to the reactor. Fig. 4 shows rates of CO conversion as a function of the time on-stream of the syngas containing $H_2S$ (100 ppm in concentration). After the syngas containing $H_2S$ was fed into the

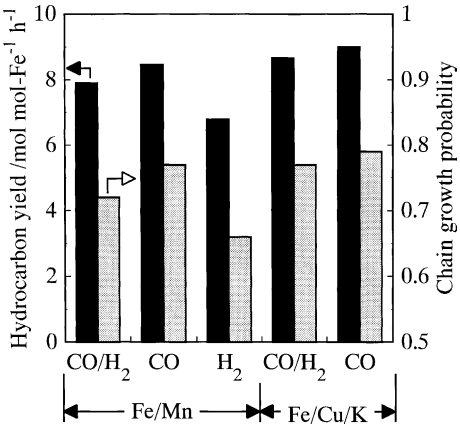


Fig. 3. Promoting effects of CO-pretreatment on the FT synthesis activities of the Fe/MnO (1/6). Reaction conditions: 33% CO/62% $H_2$/5% Ar, 523 K, 1.6 MPa.

reactor, the rate of CO conversions over the Fe/MnO (1/6) catalysts decrease gradually and are 80% of the initial value at the time on-stream of 10 h irrespective of the composition of the pretreatment gas (CO or syngas). On the other hand, the rates of CO conversion over the Fe/Cu/K catalysts decreases quickly and drops to almost 0 at the time on-stream of 10 h. Thus the CO pretreatment is effective for increasing the hydrocarbon synthesis activity of the Fe/MnO catalyst while the CO pretreatment has little influence on its superior sulfur resistance.

### 2.2.2. Surface fine structure [26]

To make clear the role of MnO, adsorption properties of surface Fe species have been investigated by DRIFT spectroscopy using CO as the surface probe molecule. The precipitated Fe and/or Fe/MnO catalyst was pretreated in a syngas stream at 573 K and 1.2 MPa for 6 h and then the catalyst was immediately cooled to room temperature. The syngas adsorption was performed using the high-pressure syngas stream at room temperature. DRIFT spectra of

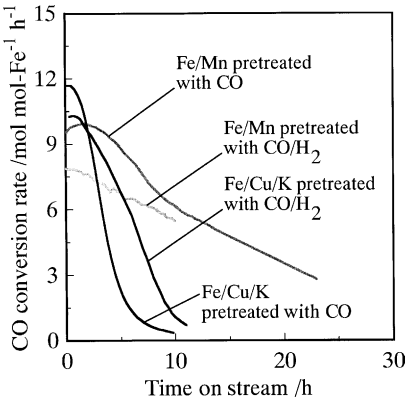


Fig. 4. Deleterious effect of $H_2S$ (100 ppm in concentration) on the rates of CO conversion over the Fe/MnO (1/6) and Fe/Cu/K catalysts pretreated with CO or CO/$H_2$. Reaction conditions: 33% CO/62% $H_2$/5% Ar, 523 K, 1.6 MPa.

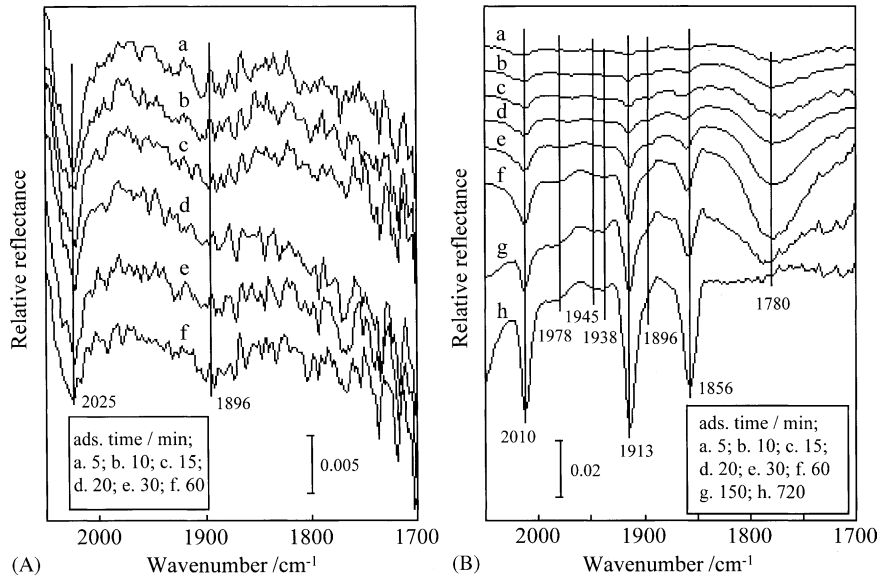


Fig. 5. Infrared spectra recorded as a function of time on-stream from the syngas adsorption on the Fe (A) and Fe/MnO (B) samples pretreated with the syngas at 573 K and 1.2 MPa for 6 h.

adsorbed CO were measured at different adsorption times. Fig. 5(A) shows the DRIFT spectra of CO adsorbed on the precipitated Fe catalyst from the syngas adsorption. During the adsorption, weak bands can be observed at 2025 and 1896 $cm^{-1}$. With increasing the adsorption time, their intensities increase slightly. Different from the Fe catalyst, a large number of distinct bands of adsorbed species are observed at 2010, 1913, 1856 and 1780 $cm^{-1}$ when the Fe/MnO (1/6) catalyst was subjected to the DRIFT measurement (Fig. 5(B)). Several weak bands can be also observed at 1978, 1945, 1938 and 1896 $cm^{-1}$.

The bands with the frequencies of 2130–2000 $cm^{-1}$ have been assigned to the linearly adsorbed CO on tops of $Fe^0$ sites and the bands of 2000–1880 $cm^{-1}$ to the two-fold bridge-bonded CO and those of 1880–1650 $cm^{-1}$ to the multiply bridge-bonded CO on deep hollow sites [27–31]. From the results mentioned above, mainly three kinds of adsorbed CO are identified on the Fe catalyst, i.e. two linear (2043 and 2025 $cm^{-1}$) and one bridged (1896 $cm^{-1}$). These bands are almost consistent with those of C–O vibrations in an iron carbonyl, $Fe_3(CO)_{12}$ (2043, 2020, 2008–1997, 1865 and 1834 $cm^{-1}$) [32]. Furthermore, no bands of CO adsorbed on the deep hollow sites are observed. It may reveal that the formed $Fe^0$ particles are composed of very small $Fe^0$ clusters. In contrast, the specific feature for the Fe/MnO (1/6) catalyst is the large number of well-resolved bands occurring upon CO adsorption. The appearance of the bands arising from the multiply bridge-bonded CO on the deep hollow site of the $Fe^0$ (1778, 1720 and 1662 $cm^{-1}$) indicates the size of the $Fe^0$ particles is relatively larger. A similar phenomenon was also observed in a Co–MnO system [33]. Since it is reasonable to assume that the increase in the size of the $Fe^0$ particles decreases its reactivity toward $H_2S$, this may be one of reasons for the superior sulfur resistance of the Fe/MnO catalyst.

## 3. Utilization of high surface area $MoS_2$ for the preparation of highly active $C_{2+}$ alcohol synthesis catalyst

Synthesis of mixed alcohols from syngas over the $MoS_2$ and/or $WS_2$-based catalysts has been studied because of their advantages of the sulfur tolerance. Patent literature [13] claimed that a K-promoted $MoS_2$ ($K/MoS_2$) yields $C_{2+}$ alcohol of 43 g $kg_{cat}^{-1}$ $h^{-1}$ at 538 K and 10.5 MPa in the presence of $H_2S$ 50 ppm in concentration. Although the higher STY of $C_{2+}$ alcohol (130 g $kg_{cat}^{-1}$ $h^{-1}$) is obtained with $Cs/MoS_2$ at 568 K and 8.2 MPa in the absence of $H_2S$ [34], this yield is still lower than that with the Cu-based catalyst (160 g $kg_{cat}^{-1}$ $h^{-1}$) [35]. The characteristic of the alcohol obtained with the $MoS_2$-based catalysts is that the formed alcohol is linear and primary alcohol whose carbon-number distribution is well matched with that predicted by Schultz–Flory kinetics. The chain growth probability of the alcohol lies in the range from 0.2 to 0.25 [13,14,34], indicating that the alcohol is mainly composed of methanol.

Several studies showed that only hydrocarbon is formed over $MoS_2$ without the alkaline metal promoters [34,36]. In other words, the alkaline metal promoter is indispensable for the alcohol formation. Mechanistic study on the alcohol formation over $Cs/MoS_2$ suggested that the chain growth of alcohol occurs through a CO insertion into adsorbed methyl intermediate to form acyl precursor [34]. It was also suggested that Cs species is responsible for the CO insertion

whereas $MoS_2$ yields dissociated hydrogen atoms. Later Lee et al. [36] found that a uniform spreading of K species over $MoS_2$ results in increasing the selectivity for $C_{2+}$ alcohol. From these results, it is expected that the chain growth of alcohol will be facilitated by a uniform spreading of the alkaline metal species over a high surface area $MoS_2$.

In the previous studies on the mixed alcohols synthesis over the Mo sulfide-based catalysts, $MoS_2$ was reported to be prepared by a thermal decomposition or reduction of $(NH_4)_2MoS_4$ (ATTM). BET surface area of $MoS_2$ thus prepared is no more than $60\,m^2\,g^{-1}$ [14,34]. On the other hand Yoneyama and Song [37] recently reported that $MoS_2$ having BET surface area of $350\,m^2\,g^{-1}$ can be prepared by the reduction of ATTM in the presence of water. However, this preparation technique has not been applied to the $MoS_2$-based mixed alcohols synthesis catalyst. To improve the $C_{2+}$ alcohol yield, a novel preparation technique was developed for the $MoS_2$-based catalyst by modifying the method reported by Yoneyama and Song. The activity of the prepared catalysts was compared with that of the conventional $MoS_2$-based catalyst.

The high surface area $MoS_2$ ($MoS_2$ (HSA)) was prepared by the reduction of ATTM dissolved into the water under a high pressure $H_2$ atmosphere in the presence of tridecane. BET surface area of $MoS_2$ (HSA) thus prepared was $220\,m^2\,g^{-1}$. An alkaline metal (M: K, Rb and Cs) promoted $MoS_2$ (HSA) was prepared using the aqueous alkaline metal carbonate solution instead of water. Over $M/MoS_2$ (HSA), alcohols composed of methanol, ethanol, propanol and butanol were formed. Fig. 6 shows STYs of $C_{2+}$ alcohol and the chain growth probabilities of alcohol with $M/MoS_2$

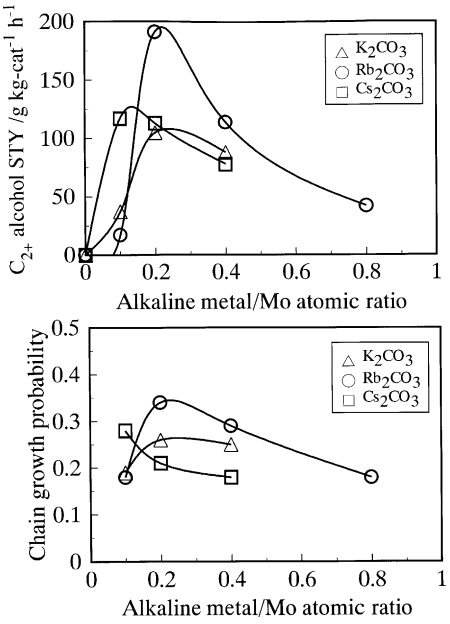


Fig. 6. Promoting effects of the alkaline metal addition on the alcohol synthesis activity of the $MoS_2$ (HSA, BET surface area: $220\,m^2\,g^{-1}$). Reaction conditions: 33% CO/62% $H_2$/5% Ar, 573 K, 5.1 MPa, $20\,m^3$ (STP) $kg_{cat}^{-1}\,h^{-1}$.

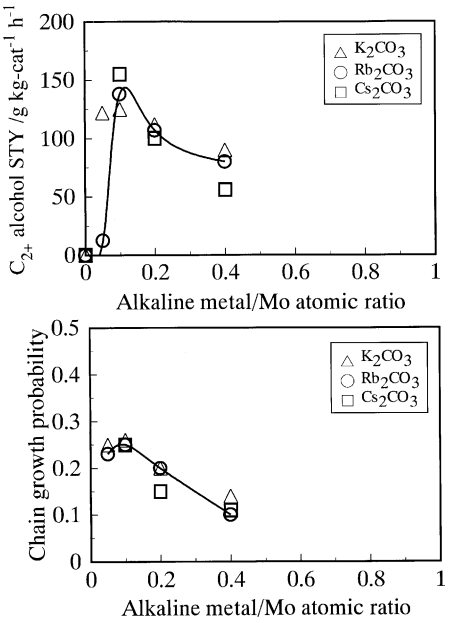


Fig. 7. Promoting effects of the alkaline metal addition on the alcohol synthesis activity of the $MoS_2$ prepared by the thermal decomposition of ATTM (BET surface area: $10\,m^2\,g^{-1}$). Reaction conditions: 33% CO/62% $H_2$/5% Ar, 573 K, 5.1 MPa, $20\,m^3$ (STP) $kg_{cat}^{-1}\,h^{-1}$.

(HSA) having various M/Mo atomic ratios. The $C_{2+}$ alcohol STY over $M/MoS_2$ (HSA) strongly depends on the M/Mo ratio and shows a maximum at the M/Mo ratio of around 0.2 irrespective of the alkaline metal promoter. Among these catalysts $Rb/MoS_2$ (HSA) having Rb/Mo ratio of 0.25 shows the highest $C_{2+}$ alcohol STY. The chain growth probability of the alcohol with this catalyst is the highest as well.

For comparison a low surface area $MoS_2$ ($MoS_2$ (LSA)) was also prepared by the thermal decomposition of ATTM (BET surface area: $10\,m^2\,g^{-1}$). The alkaline metal promoter was added by mixing $MoS_2$ (LSA) with the alkali metal carbonate using a mortar and pestle. Results of catalytic activity tests with $M/MoS_2$ (LSA) are shown in Fig. 7. The highest STY and chain growth probability are obtained with the Cs promoted catalyst in the case of $MoS_2$ (LSA)-based catalyst, which is consistent with the previous literature [34]. These values are, however, obviously lower than those with the $Rb/MoS_2$ (HSA). From the results shown here, it is suggested that the uniform spreading of the Rb promoter facilitates the chain growth of alcohol, which will result in the increase of the $C_{2+}$ alcohol yield. It should be also noted that the $C_{2+}$ alcohol STY over the $Rb/MoS_2$ (HSA) having Rb/Mo atomic ratio of 0.25 is also higher than that with the Cu-based catalyst [35].

## 4. CO hydrogenation activity and selectivity of transition metal sulfides

As was already shown by the previous studies [13,14] both Mo and W sulfide-based catalysts show the excellent

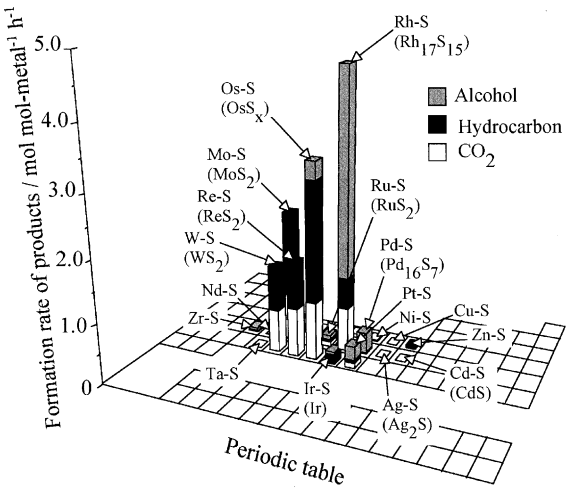


Fig. 8. Formation rates of products over various metal sulfide samples. Parentheses indicate the crystalline structures of the metal sulfides before the reaction determined with the powder XRD method. Reaction conditions, 33% CO/62% $H_2$/5% Ar, 613 K, 5.1 MPa.

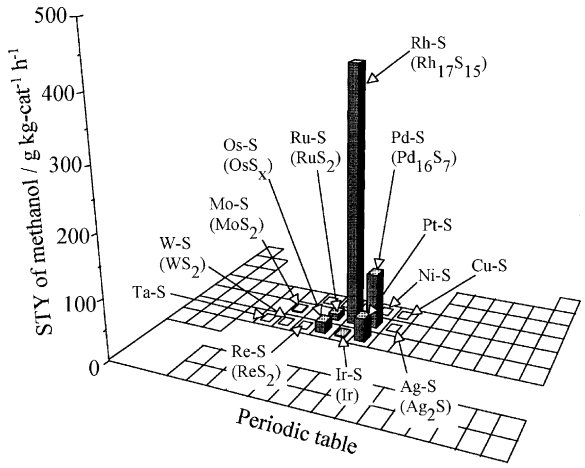


Fig. 9. STY of methanol obtained with various metal sulfide samples. Reaction conditions: 33% CO/62% $H_2$/5% Ar, 613 K, 5.1 MPa.

sulfur tolerances in the mixed alcohols synthesis. These results imply that the application of transition metal sulfides is a most promising way to develop the sulfur tolerant catalyst for the CO hydrogenation. However, CO hydrogenation activities and selectivities of the transition metal sulfides other than Mo and W sulfides have never been investigated yet. To find novel metal sulfides that are active and selective for the CO hydrogenation, various bulk sulfides were prepared and their activities and selectivities were investigated.

Metal sulfides were prepared by a modified manner reported by Pecoraro and Chianelli [38]. Sulfiding treatments were performed in a stream of 5% $H_2S/H_2$ instead of pure $H_2S$ used in the literature. Before the CO hydrogenation reaction the metal sulfide was sulfided in situ in a stream of 0.1% $H_2S/H_2$ at 673 K again and then subjected to the reaction at 613 K and 5.1 MPa. Fig. 8 shows formation rates of products obtained with the various metal sulfides. $MoS_2$ and $WS_2$ without the alkaline metal promoters yield $C_1$–$C_3$ alkane as hydrogenated products, which is consistent with the previous studies [34,36]. In addition to these metal sulfides, Rh, Pd, Re and Os sulfides show CO hydrogenation activities as well. Especially, the Rh sulfide and the Os sulfide show the higher CO hydrogenation activities (sum of the formation rate of the products except for $CO_2$) than Mo and W sulfides. As shown in the figure, the Os sulfide mainly yields $C_1$–$C_4$ alkane whereas the main product obtained with the Rh, Pd and Pt sulfides was methanol [39,40]. Especially both the Pd sulfide and the Pt sulfide yield methanol selectively. The methanol selectivities of these sulfides are above 90 C-mol%. In Fig. 9 STYs of methanol obtained with the metal sulfides are shown. The STY of methanol with the Rh sulfide is much higher (420 g $kg_{cat}^{-1}$ $h^{-1}$) than those with the other metal sulfides. Since the alkaline metal promoted $MoS_2$ (HSA) yielded less than 300 g $kg_{cat}^{-1}$ $h^{-1}$ of methanol, the Rh sulfide shows the higher methanol synthesis activity than the $MoS_2$-based alcohol synthesis catalyst.

To determine the crystalline structure of the Rh and Pd sulfides, powder X-ray diffraction (XRD) patterns of the sulfides before and after the reaction were measured. For Rh–S system, $Rh_{17}S_{15}$ [41], $Rh_3S_4$ [42] and $Rh_2S_3$ [43] have been synthesized from the metallic Rh powder and S vapor at temperatures above 1000 K and their structural parameters have been determined by XRD method. By using these parameters, relative intensities of the diffraction peaks of $Rh_{17}S_{15}$, $Rh_3S_4$ and $Rh_2S_3$ were calculated and were compared with that of the Rh sulfide. It was revealed that the relative intensities of the diffraction peaks of the Rh sulfides before and after the reaction match well with that of $Rh_{17}S_{15}$. Thus, the crystalline structure of the Rh sulfide before the reaction is $Rh_{17}S_{15}$ and the $Rh_{17}S_{15}$ structure is maintained during the reaction at 613 K and 5.1 MPa. The crystalline structures of the Pd sulfides before and after the reaction were also determined to be $Pd_{16}S_{17}$ and $Pd_4S$, respectively, in the same manner. In other words, XRD measurements indicated that the structural change occurs during the reaction in the case of the Pd sulfide. The structural change of the Pd sulfide was also confirmed by means of in situ EXAFS measurements and the thermodynamic equilibrium considerations.

## 5. Improvement of the methanol synthesis activities of the Rh and Pd sulfides

Methanol is currently synthesized from the syngas derived from natural gas using a Cu/ZnO-type catalyst. Before 1960 a $ZnO/Cr_2O_3$ catalyst that shows the superior sulfur resistance than the Cu/ZnO catalyst [2] was used because the syngas derived from coal was used as the feed. In the last section, several bulk sulfides were found to show the CO hydrogenation activities. In particular, both the Rh and Pd sulfides are active and selective for the methanol

synthesis. To improve their methanol synthesis activities, effects of supports and additives were further investigated. The activities of these sulfides were then compared with those of the $ZnO/Cr_2O_3$ and the $Cu/ZnO/Al_2O_3$ catalysts in the absence and presence of $H_2S$.

### 5.1. Rh sulfide

#### 5.1.1. Effect of the support

Rh catalysts reduced by $H_2$ are well known to show a catalytic activity for the conversion of the syngas. Ichikawa [44] reported that methanol is formed selectively when an alkaline earth metal oxide or ZnO is used as a support whereas a reduced $Rh/SiO_2$ yields hydrocarbons exclusively. The addition of Ti [45], Mn [46], Fe [47] and/or Zr [45] oxide to the reduced $Rh/SiO_2$ improves the formation rate of methanol as well as ethanol. In situ XPS measurements showed that Rh species supported on $SiO_2$ after the $H_2$ reduction is in a metallic state while those on ZnO support is in a cationic state [48]. Ponec and coworkers [49] found that the methanol selectivity of the supported catalysts increases with increasing the extractable amount of the cationic Rh species, which leads them to the hypothesis that the cationic Rh species are active for the methanol formation [49,50]. The importance of cationic Rh sites in the higher alcohol synthesis has been also pointed out by Chuang and coworkers. They found that both $Rh^0$ atoms and cationic Rh atoms over the reduced and oxidized $Rh/SiO_2$ are active for the CO insertion in the ethylene hydroformylation that yields propionaldehyde by in situ IR spectroscopy [51]. They also found that some supported sulfides such as sulfided $Ni/SiO_2$ catalyze the CO insertion at high-pressure reaction conditions [52]. The CO insertion is believed to be a key step for the higher alcohol synthesis. From these previous works, it is suggested that the cationic Rh sites are stabilized by Rh–S bonds in Rh sulfide ($Rh_{17}S_{15}$) and are active for the methanol formation. Therefore it is possible that there appear several differences in the selectivity for the CO hydrogenation between the supported reduced Rh catalysts and supported Rh sulfides. It is also expected that the supported Rh sulfides show higher activities than the bulk Rh sulfide since the supported Rh sulfides may be in highly dispersed states. For these reasons, activities and selectivities of Rh sulfide dispersed on various supports for CO hydrogenation were investigated.

Rh oxide supported on various support materials (Rh content: 5 mass%) was prepared by the incipient wetness method and then sulfided in a stream of 5% $H_2S/H_2$ at 673 K before the reaction. Fig. 10 shows the rate of CO conversion (A), the product selectivity (B) and the STY of alcohol (C) obtained with the supported Rh sulfide. The rate of CO conversion over a sulfided $Rh/TiO_2$ is the highest whereas the products are exclusively hydrocarbon and $CO_2$. Similar product selectivity is obtained with a sulfided $Rh/Al_2O_3$. On the other hand, methanol is formed as a main product when $SiO_2$, MgO and/or active carbon are used as the support. Methanol selectivity of a sulfided $Rh/SiO_2$ decreases with

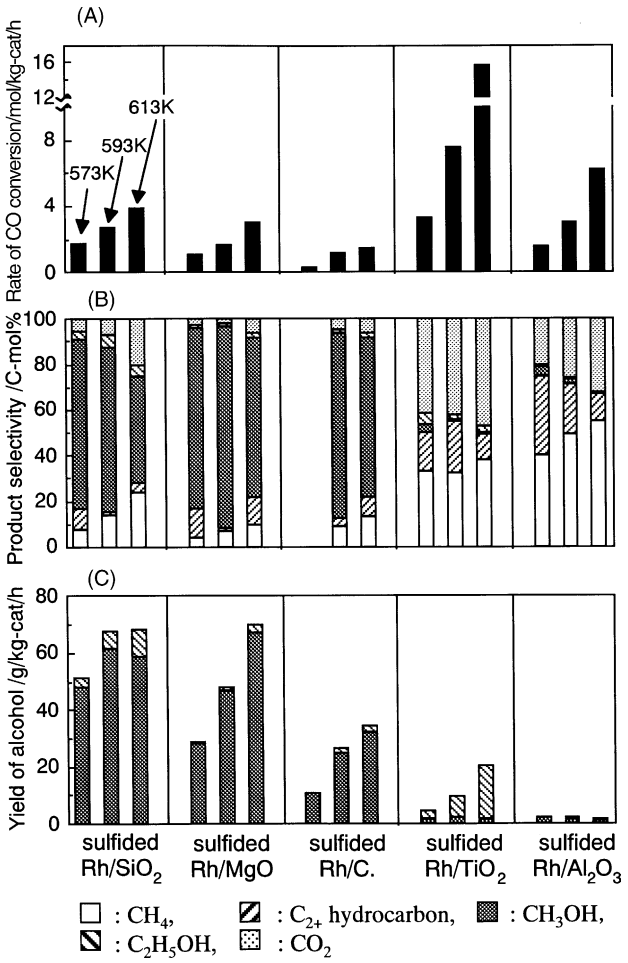


Fig. 10. Rate of CO conversion (A), product selectivity (B) and yield of alcohol (C) obtained with the supported Rh sulfide catalysts. Reaction conditions: 33% CO/62% $H_2$/5% Ar, 573 K (or 593, 613 K), 5.1 MPa, 10 $m^3$ (STP) $kg_{cat}^{-1}$ $h^{-1}$.

increasing the reaction temperature (50 C-mol% at 613 K). In the case of both the sulfided Rh/MgO and the sulfided Rh/C, the methanol selectivites are above 70 C-mol% irrespective of the reaction temperature. It should be noted that the reduced $Rh/SiO_2$ is reported to yield the hydrocarbon exclusively [44] whereas the sulfided $Rh/SiO_2$ mainly yields methanol. Such a difference will explain if the cationic Rh sites are stabilized by Rh–S bonds under the reaction conditions, which supports our hypothesis mentioned above. Besides the methanol STY over the sulfided $Rh/SiO_2$ at 613 K normalized to the total Rh atoms was 2.0 times higher than the bulk Rh sulfide although the STY of methanol with the sulfided $Rh/SiO_2$ was lower.

#### 5.1.2. Comparison with the reduced Fe-Rh/$SiO_2$ catalyst

Among the reduced Rh catalysts reported so far, the reduced Fe-$Rh/SiO_2$ catalyst shows the highest methanol synthesis activity (167 g $kg_{cat}^{-1}$ $h^{-1}$ of methanol at 573 K and 6.9 MPa) [47]. In this paragraph, the methanol synthesis activity of the bulk Rh sulfide is compared with that of the

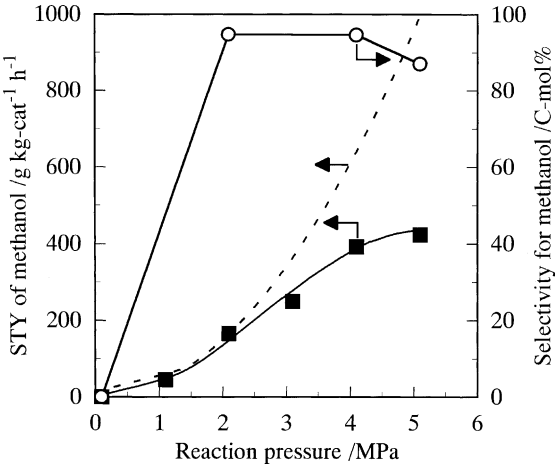


Fig. 11. Effect of reaction pressure on STY (■) and selectivity (○) of methanol obtained with $Rh_{17}S_{15}$. Reaction conditions: 33% CO/62% $H_2$/5% Ar, 613 K, 30 m$^3$ (STP) kg$_{cat}^{-1}$ h$^{-1}$.

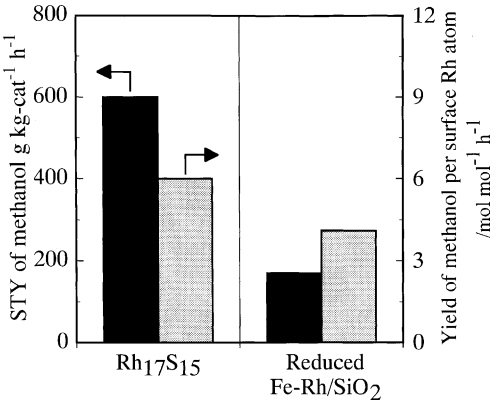


Fig. 13. Comparison of the methanol synthesis activity of $Rh_{17}S_{15}$ and the reduced Fe-Rh/$SiO_2$ catalyst [47]. Reaction conditions: 33% CO/62% $H_2$/5% Ar, 573 K, 5.1 MPa, 30 m$^3$ (STP) kg$_{cat}^{-1}$ h$^{-1}$ for $Rh_{17}S_{15}$ and 50% CO/50% $H_2$, 573 K, 5.1 MPa, 39 m$^3$ (STP) kg$_{cat}^{-1}$ h$^{-1}$ for the reduced Fe-Rh/$SiO_2$ catalyst.

reduced Fe-Rh/$SiO_2$. Before comparison, effects of reaction pressure and temperature on methanol STY and selectivity of $Rh_{17}S_{15}$ are investigated (Figs. 11 and 12). $Rh_{17}S_{15}$ was pretreated with 0.1% $H_2S/H_2$ and subjected to the reaction. At atmospheric pressure, no methanol is formed (Fig. 11). Methanol is formed at the pressure of 1.1 MPa or above, and the methanol STY increases with increasing the reaction pressure up to 5.1 MPa (590 g kg$_{cat}^{-1}$ h$^{-1}$ at 5.1 MPa). The methanol STYs at 1.1 and 2.1 MPa are nearly equal to the equilibrium values whereas the methanol STYs above 2.1 MPa are lower than the equilibrium values. Methanol selectivity is above 80 C-mol% when the pressure lies in a range from 2.1 to 5.1 MPa. Fig. 12 shows methanol STY and selectivity at 5.1 MPa as a function of reaction temperature. As shown in this figure, STY of methanol increases with increasing the reaction temperature up to 593 K. The STY does not change when the reaction temperature increases from 593 to 613 K. Methanol selectivity decreases with increasing the reaction temperature because of the thermodynamic equilibrium. Among $Rh_{17}S_{15}$ pretreated with $H_2S/H_2$ having various $H_2S$ concentrations, $Rh_{17}S_{15}$ pretreated with 0.5% $H_2S/H_2$ showed the highest STY, which was 1.5 times higher than that obtained with $Rh_{17}S_{15}$ shown in Fig. 12. Fig. 13 shows STYs with $Rh_{17}S_{15}$ and the reduced Fe-Rh/$SiO_2$. $Rh_{17}S_{15}$ pretreated with 0.5% $H_2S/H_2$ yields 600 g kg$_{cat}^{-1}$ h$^{-1}$ of methanol at 573 K and 5.1 MPa. In other words the higher methanol STY can be obtained with $Rh_{17}S_{15}$ even at the lower reaction pressure. To compare the intrinsic activities of these catalysts, a CO uptake of $Rh_{17}S_{15}$ was measured and then the methanol yield normalized to the surface Rh atoms was calculated. The result is also shown in Fig. 13. The methanol yield over $Rh_{17}S_{15}$ normalized to the surface Rh atoms are obviously higher than that reported for the reduced Fe-Rh/$SiO_2$ [47], indicating that the cationic Rh sites stabilized by the Rh–S bonds are much more effective for the methanol formation than those of the reduced Rh catalysts.

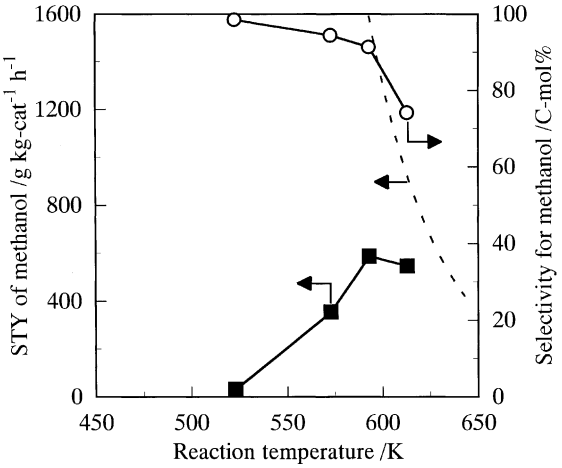


Fig. 12. Effect of reaction temperature on STY (■) and selectivity (○) of methanol obtained with $Rh_{17}S_{15}$. Reaction conditions: 33% CO/62% $H_2$/5% Ar, 5.1 MPa, 30 m$^3$ (STP) kg$_{cat}^{-1}$ h$^{-1}$.

## 5.2. Pd sulfide

### 5.2.1. Effect of the support [40,53]

Before our study, $H_2$-reduced Pd catalysts supported on some metal oxides are known to yield methanol selectively [54]. Especially $La_2O_3$ [55] $CeO_2$ [56] and $Nd_2O_3$ [55] are effective supports for the selective methanol synthesis. Thus methanol synthesis activities of Pd sulfides supported on various metal oxides have been investigated.

Pd oxide supported on $M_xO_y$ (M: Mg, Al, Si, Ca, Zr, La, Ce and Nd, Pd content: 5 mass%) was prepared by the incipient wetness method and then sulfided in a stream of 5% $H_2S/H_2$ at 673 K before the reaction. Fig. 14 summarizes STYs of methanol obtained with sulfided Pd/$M_xO_y$ and the bulk Pd sulfide ($Pd_{16}S_7$) at 613 K and 5.1 MPa.

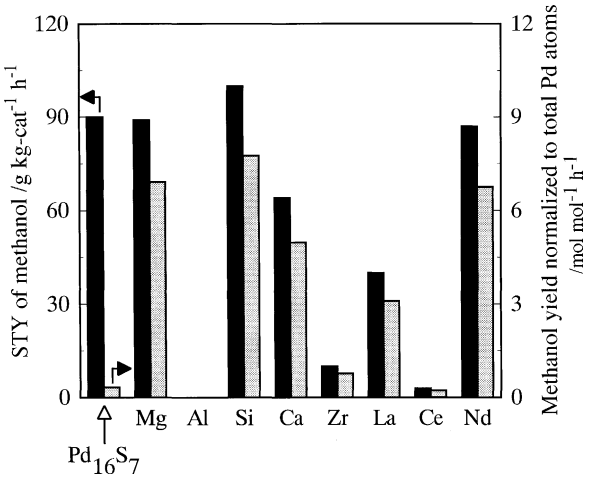


Fig. 14. Effects of oxide supports ($M_xO_y$, M: Mg, Al, Si, Ca, Zr, La, Ce, Nd) on the methanol synthesis activity of Pd sulfide. Reaction conditions: 33% CO/62% $H_2$/5% Ar, 613 K, 5.1 MPa, 20 $m^3$ (STP) $kg_{cat}^{-1}$ $h^{-1}$.

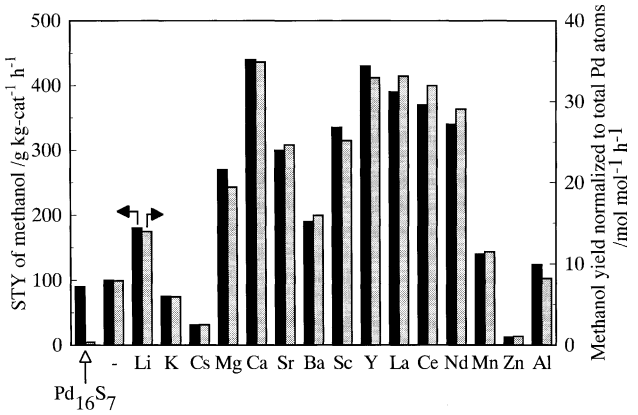


Fig. 15. Effects of various additives (M: Li, K, Cs, Mg, Ca, Sr, Ba, Sc, Y, La, Ce, Nd, Mn, Zn, Al, M/Pd atomic ratio: 0.5) on the methanol synthesis activity of sulfided $Pd/SiO_2$. Reaction conditions: 33% CO/62% $H_2$/5% Ar, 613 K, 5.1 MPa, 20 $m^3$ (STP) $kg_{cat}^{-1}$ $h^{-1}$.

This figure also shows methanol STYs normalized to the total Pd atoms. Pd sulfides supported on MgO, $SiO_2$, CaO, $La_2O_3$, $CeO_2$ and/or $Nd_2O_3$ yielded mainly methanol whereas $CH_4$ was a main product when $ZrO_2$ and $CeO_2$ are utilized as the support. Over sulfided $Pd/Al_2O_3$ only $CH_4$ and $CO_2$ were formed. The STY of methanol with the supported Pd sulfides decreases as a following order: sulfided $Pd/SiO_2$ > sulfided $Pd/Nd_2O_3$ > sulfided Pd/MgO > sulfided Pd/CaO > sulfided $Pd/La_2O_3$ > sulfided $Pd/ZrO_2$ > sulfided $Pd/CeO_2$.

The STY of methanol with sulfided $Pd/SiO_2$ is 1.1 times higher than that with $Pd_{16}S_7$. On the other hand, the methanol STY over the sulfided $Pd/SiO_2$ normalized to the total Pd atoms is about 20 times higher than that over $Pd_{16}S_7$. This indicates that the Pd sulfide on $SiO_2$ support is in a highly dispersed state and effectively involved in the formation of methanol than the bulk sulfide.

### 5.2.2. *Effect of the additive on the methanol synthesis activity of sulfided $Pd/SiO_2$ [57]*

Then methanol synthesis activities of sulfided $Pd/SiO_2$ doped with various metal additives have been investigated because the methanol synthesis activity of a reduced $Pd/SiO_2$ is greatly improved by the addition of some metal oxides [58,59]. Effects of the preparation method for the oxide precursor were also examined.

$PdO/SiO_2$ was doped with an aqueous metal (M: Li, K, Cs, Mg, Ca, Sr, Ba, Sc, Y, La, Ce, Nd, Mn, Zn and Al) nitrate solution followed by drying and then sulfided before the reaction. Most of additives examined here increased the STY of methanol with the sulfided $Pd/SiO_2$. The STY of methanol with the sulfided $M/Pd/SiO_2$ sharply increased with increasing the M/Pd atomic ratio up to 0.5 and showed plateaus at above this ratio. Fig. 15 shows STYs of methanol with sulfided $M/Pd/SiO_2$ having the M/Pd atomic ratio of 0.5 as well as the bulk Pd sulfide. This figure also shows methanol STYs normalized to the total Pd atoms. The highest methanol STY is obtained with the sulfided $Ca/Pd/SiO_2$ and is about five times higher than that with $Pd_{16}S_7$. The methanol STY over the sulfided $Ca/Pd/SiO_2$ normalized to the total Pd atoms is about 100 times higher than that with the bulk sulfide. Thus the utilization of the $SiO_2$ support and the addition of Ca are quite effective for the improvement in the methanol synthesis activity of the bulk sulfide. Effects of reaction pressure and temperature on methanol STY and selectivity of the sulfided $Ca/Pd/SiO_2$ are also investigated (Figs. 16 and 17). Different from $Rh_{17}S_{15}$, methanol is formed selectively (80 C-mol%) even at the atmospheric pressure (Fig. 16). The methanol STY increases with increasing the reaction pressure up to 5.1 MPa. The methanol STYs at the atmospheric pressure and 2.1 MPa are nearly equal to the equilibrium values whereas the methanol STYs above 1.1 MPa are lower than the equilibrium values. The

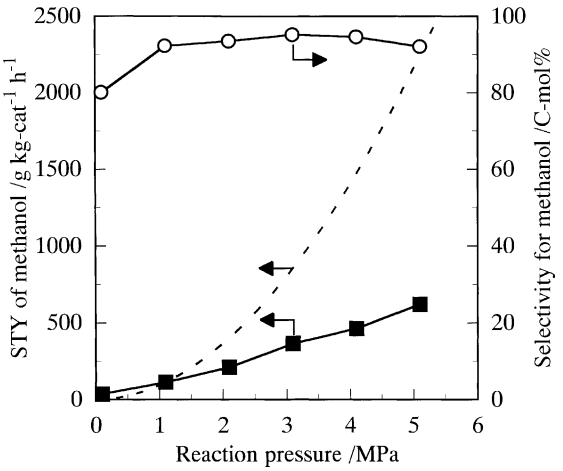


Fig. 16. Effect of reaction pressure on STY (■) and selectivity (○) of methanol obtained with sulfided $Ca/Pd/SiO_2$. Reaction conditions: 33% CO/62% $H_2$/5% Ar, 593 K, 30 $m^3$ (STP) $kg_{cat}^{-1}$ $h^{-1}$.

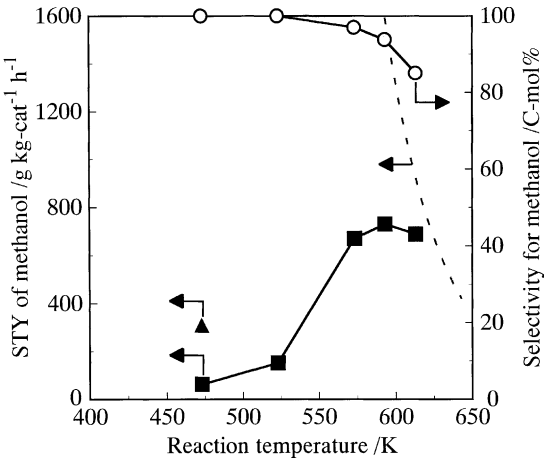


Fig. 17. Effect of reaction temperature on STY (■) and selectivity (○) of methanol obtained with sulfided $Ca/Pd/SiO_2$. For comparison purpose, STY of methanol obtained with the reduced $Pd/CeO_2$ (▲) is also shown. Reaction conditions: 33% CO/62% $H_2$/5% Ar, 5.1 MPa, 30 $m^3$ (STP) $kg_{cat}^{-1}$ $h^{-1}$ for sulfided $Ca/Pd/SiO_2$; 33% CO/67% $H_2$, 2.0 MPa, 3.6 $m^3$ (STP) $kg_{cat}^{-1}$ $h^{-1}$ for the reduced $Pd/CeO_2$ [56].

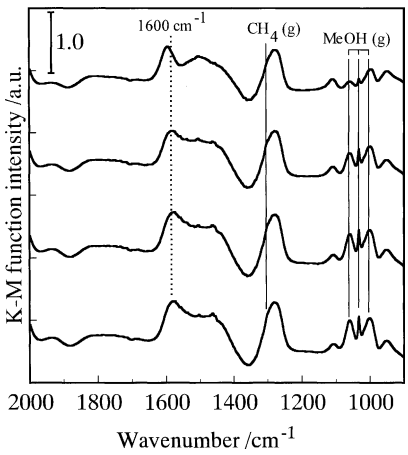


Fig. 18. DRIFT spectra of sulfided $Ca/Pd/SiO_2$ having Ca/Pd atomic ratio of 0.5 under the high-pressure methanol synthesis conditions as a function of time-on stream (from top to bottom, $t$ = 0, 30, 90, 150 min).

methanol selectivity is above 90 °C mol% when the reaction pressure is in a range from 1.1 to 5.1 MPa. As concerns the effect of the reaction temperature (Fig. 17), STY of methanol and selectivity of the sulfided $Ca/Pd/SiO_2$ exhibit trends similar to those of $Rh_{17}S_{15}$, respectively.

Among the reduced Pd catalysts reported so far, a reduced $Pd/CeO_2$ catalyst shows the highest methanol synthesis activity especially at the lower reaction temperatures [56]. So the methanol synthesis activity of the sulfided $Ca/Pd/SiO_2$ is compared with that of the reduced $Pd/CeO_2$ catalyst (Fig. 17). According to the literature [56], the reduced $Pd/CeO_2$ catalyst yields 310 g $kg_{cat}^{-1}$ $h^{-1}$ of methanol at 473 K and 2.0 MPa whereas the STY of methanol with the sulfided $Ca/Pd/SiO_2$ is 60 g $kg_{cat}^{-1}$ $h^{-1}$ at the same reaction temperature. The STY of methanol with the supported sulfide is no more than 20% of that with the reduced catalyst. However, since Pd content of the reduced $Pd/CeO_2$ catalyst is 3.7 times higher than that of the sulfided $Ca/Pd/SiO_2$, the methanol STY over the supported sulfide normalized to the total Pd atoms reaches 75% of that with the reduced catalyst.

### 5.2.3. Role of the Ca additive

In the methanol synthesis over the reduced Pd catalyst promoted with the Ca and/or Mg additive it is suggested that the metal additive stabilizes the reaction intermediate such as a formyl [60] or a formate [58,59] species. To examine the role of the Ca additive in the methanol synthesis over the sulfided $Ca/Pd/SiO_2$, DRIFT spectra of the adsorbed species over the sulfided catalyst under the high-pressure methanol synthesis conditions were investigated. DRIFT spectra were recorded as a function of time when the sulfided $Ca/Pd/SiO_2$ was exposed to the stream of the syngas at 613 K and 5.1 MPa (Fig. 18).

In addition to the bands assigned to the gas-phase methanol and methane (see Fig. 18), several bands are clearly observed in the spectra. To facilitate the assignment of these bands, the reaction temperature was reached down to 298 K and then the chamber was flushed with a helium flow. Although the bands of the gas-phase products completely disappeared, the bands at 1600 and 1270 $cm^{-1}$ were still visible. Several authors have reported that IR bands of adsorbed formate species are observed when reduced Pd catalysts are exposed to the stream of the syngas at elevated temperatures [59,61]. The formate species yields IR bands at 1600–1550, 1400–1380, 1380–1340 and 1090–1060 $cm^{-1}$ [62]. The band at 1600 $cm^{-1}$ shown in Fig. 18, therefore, can be assigned to the formate species. It should be noted that the spectra show no IR bands at around 1700 $cm^{-1}$ although the band assigned to the formyl species appears at 1748 $cm^{-1}$ when the reduced $Ca/Pd/SiO_2$ is exposed to the methanol vapor at room temperature [63]. The appearance of the band at 1450 $cm^{-1}$ also suggests the formation of methoxy or methyl species.

As mentioned in the last paragraph, the methanol synthesis activity of the sulfided $Ca/Pd/SiO_2$ increases with increasing Ca/Pd atomic ratio up to 0.5. So, the dependency of the intensity of the formate band on the Ca/Pd atomic ratio was examined. Fig. 19 shows DRIFT spectra of sulfided $Ca/Pd/SiO_2$ with various Ca/Pd atomic ratios. The intensity of the formate band (at around 1600 $cm^{-1}$) increases with increasing the Ca/Pd ratio. Thus it is suggested that the formate species is the reaction intermediate for the methanol formation over the sulfided $Ca/Pd/SiO_2$ and the Ca additive stabilizes the formate species.

### 5.3. Comparison with the $ZnO/Cr_2O_3$ and $Cu/ZnO/Al_2O_3$ catalysts

In this paragraph, the methanol synthesis activities of $Rh_{17}S_{15}$ and the sulfided $Ca/Pd/SiO_2$ are compared with

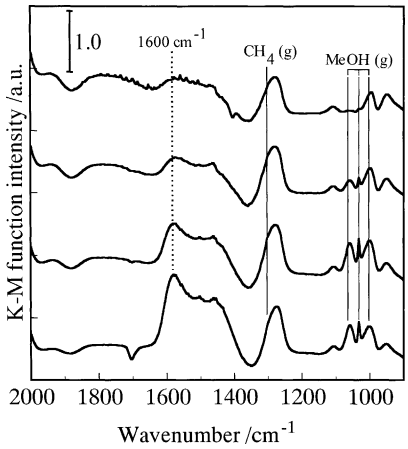


Fig. 19. DRIFT spectra of sulfided $Ca/Pd/SiO_2$ having various Ca/Pd atomic ratios under the high-pressure methanol synthesis conditions (from top to bottom, Ca/Pd atomic ratio = 0, 0.1, 0.5, 1.0).

those of the $ZnO/Cr_2O_3$ and the $Cu/ZnO/Al_2O_3$ catalysts. Fig. 20 shows STYs of methanol obtained with $Rh_{17}S_{15}$ and the sulfided $Ca/Pd/SiO_2$ as a function of the reaction temperature. Dashed lines indicate equilibrium methanol STYs at each reaction temperature with a gas hourly space velocity of 30 $m^3$ (STP) $kg_{cat}^{-1}$ $h^{-1}$ (···) and 6 $m^3$ (STP) $kg_{cat}^{-1}$ $h^{-1}$ (----). At 30 $m^3$ (STP) $kg_{cat}^{-1}$ $h^{-1}$, the STYs of methanol with both $Rh_{17}S_{15}$ and the sulfided $Ca/Pd/SiO_2$ show a maximum at 593 K. The STYs of methanol with $Rh_{17}S_{15}$ and the sulfided $Ca/Pd/SiO_2$ at this reaction temperature are 820 and 730 g $kg_{cat}^{-1}$ $h^{-1}$, respectively. Being normalized by the total amount of Pd or Rh atoms, the formation rate of methanol over the sulfided $Ca/Pd/SiO_2$ is ca. 18 times higher than that over $Rh_{17}S_{15}$. Thus the sulfided $Ca/Pd/SiO_2$ is more suitable than the $Rh_{17}S_{15}$ from economic points of view.

Fig. 20 also shows the results obtained with the $ZnO/Cr_2O_3$ catalyst and the commercial $Cu/ZnO/Al_2O_3$ catalyst (supplied by ICI Corp.). At 593 K and 30 $m^3$ (STP) $kg_{cat}^{-1}$ $h^{-1}$ the STY of methanol with the $ZnO/Cr_2O_3$ catalyst is much lower than that with the sulfide sample. For the commercial $Cu/ZnO/Al_2O_3$ catalyst, the feed containing both the syngas and $CO_2$ was used here because it is well known that small amounts of $CO_2$ in the feed greatly improves its methanol synthesis activity [64]. At 593 K and 30 $m^3$ (STP) $kg_{cat}^{-1}$ $h^{-1}$, the STY of methanol with the $Cu/ZnO/Al_2O_3$ catalyst is much higher than that with the sulfide sample and reaches the equilibrium value. At 523 K and 6 $m^3$ (STP) $kg_{cat}^{-1}$ $h^{-1}$ where the $Cu/ZnO/Al_2O_3$ catalyst is usually used, the methanol STY is 1200 g $kg_{cat}^{-1}$ $h^{-1}$, which is still higher than that with the sulfide sample.

Then, effects of $H_2S$ were examined. After the methanol synthesis activities of each catalyst reached steady states under the sulfur-free conditions, the syngas mixed with 0.1% $H_2S/H_2$ was fed to the reactor. Methanol STYs as a function of the total amount of $H_2S$ fed during the reactions are shown in Fig. 21. The total amount of $H_2S$ shown in the figure is normalized to the total metal content of the catalyst. Soon after the syngas containing $H_2S$ ($H_2S$ concentration: 120 ppm) was fed into the reactor, the STY over the sulfided $Ca/Pd/SiO_2$ decreases to 35% of the initial value. Thereafter, this catalyst preserves a constant STY, i.e. 250 g $kg_{cat}^{-1}$ $h^{-1}$ even when the total amount of $H_2S$ reaches 6.0 mol $H_2S$ mol $Pd^{-1}$. On the other hand, $Rh_{17}S_{15}$ preserves the initial activity irrespective of the total amount of $H_2S$ fed during the reaction. In marked contrast to the sulfide samples, the STYs of methanol with the $ZnO/Cr_2O_3$ catalyst and the commercial $Cu/ZnO/Al_2O_3$ catalyst de-

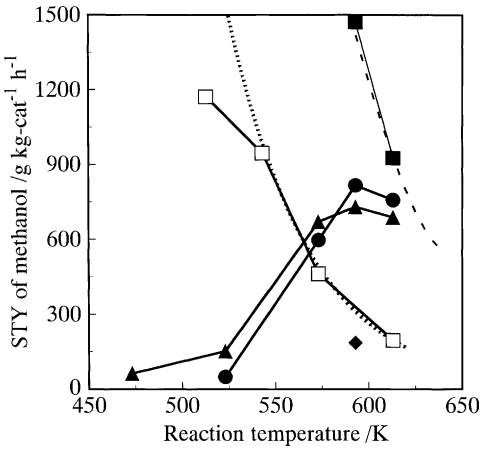


Fig. 20. STY of methanol obtained with sulfide catalysts, $ZnO/Cr_2O_3$ catalyst and the commercial $Cu/ZnO/Al_2O_3$ catalyst as a function of the reaction temperature. Reaction conditions, 33% CO/62% $H_2$/5% Ar, 5.1 MPa, 30 $m^3$ (STP) $kg_{cat}^{-1}$ $h^{-1}$ for $Rh_{17}S_{15}$ (●), sulfided $Ca/Pd/SiO_2$ (▲) and $ZnO/Cr_2O_3$ catalyst (◆), 30% CO/60% $H_2$/5% $CO_2$/5% Ar, 5.1 MPa, 6.0 $m^3$ (STP) $kg_{cat}^{-1}$ $h^{-1}$ (□) or 30 $m^3$ (STP) $kg_{cat}^{-1}$ $h^{-1}$ (■) for the $Cu/ZnO/Al_2O_3$ catalyst.

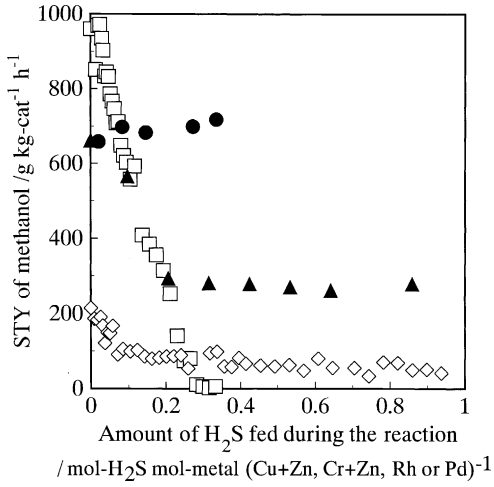


Fig. 21. Effect of $H_2S$ on STY of methanol obtained with sulfide catalysts, $ZnO/Cr_2O_3$ catalyst and the commercial $Cu/ZnO/Al_2O_3$ catalyst. Reaction conditions: 33% CO/62% $H_2$/5% Ar, 613 K, 5.1 MPa, 30 $m^3$ (STP) $kg_{cat}^{-1}$ $h^{-1}$ for $Rh_{17}S_{15}$ (●); 33% CO/62% $H_2$/5% Ar, 593 K, 5.1 MPa, 30 $m^3$ (STP) $kg_{cat}^{-1}$ $h^{-1}$ for sulfided $Ca/Pd/SiO_2$ (▲) and $ZnO/Cr_2O_3$ catalyst (◇); 30% CO/60% $H_2$/5% $CO_2$/5% Ar, 523 K, 5.1 MPa, 6.0 $m^3$ (STP) $kg_{cat}^{-1}$ $h^{-1}$ for the $Cu/ZnO/Al_2O_3$ catalyst (□).

crease with increasing the total amounts of $H_2S$ fed during the reaction. Especially, the STY over the $Cu/ZnO/Al_2O_3$ catalyst decreases much more rapidly compared with the $ZnO/Cr_2O_3$ catalyst and eventually drops into 0 at about 0.3 mol $H_2S$ mol$^{-1}$ (Cu + Zn). In other words both $Rh_{17}S_{15}$ and the sulfided $Ca/Pd/SiO_2$ have much superior sulfur tolerances than the $ZnO/Cr_2O_3$ and $Cu/ZnO/Al_2O_3$ catalysts.

## 6. In situ DME synthesis over the sulfided $Ca/Pd/SiO_2$ mixed with a solid acid from the syngas containing $H_2S$

As shown in Fig. 17, the STY of methanol obtained with the sulfided Ca–$Pd/SiO_2$ shows the maximum at 593 K. The methanol STY slightly decreases when the reaction temperature increases from 593 to 613 K because of the thermodynamic equilibrium. Thus it is necessary for a further increase of the methanol STY over the sulfided $Ca/Pd/SiO_2$ to improve the methanol synthesis activity at the lower temperatures or to avoid the thermodynamic equilibrium at the higher temperature. In situ DME synthesis is one of most promising way to avoid the thermodynamic equilibrium for the methanol synthesis. Furthermore, DME is the high quality transportation fuel for the diesel vehicles. Thus the authors have tried in situ DME synthesis over the sulfided $Ca/Pd/SiO_2$ mixed with a solid acid. The possibility of in situ DME synthesis from the syngas containing $H_2S$ has been also examined.

Effects of several solid acids on the product selectivity were investigated at first when the sulfided $Ca/Pd/SiO_2$ mixed with the solid acid was subjected to the syngas reaction. γ-$Al_2O_3$, β-zeolite, mordenite, Y-zeolite and L-zeolite were tested as the solid acids. The $Ca/PdO/SiO_2$ mixed with the solid acid was sulfided before the reaction in the stream of 5% $H_2S/H_2$ at 673 K and then subjected to the syngas reaction at 613 K and 5.1 MPa in the absence of $H_2S$. Our results showed that DME is formed in the presence of γ-$Al_2O_3$, β-zeolite and/or Y-zeolite and γ-$Al_2O_3$ was the most effective among them. The total STY of DME (equivalent to methanol) and a small amount of methanol with the sulfided $Ca/Pd/SiO_2$ mixed with γ-$Al_2O_3$ was 1.5 times higher than the equilibrium methanol STY. The STY of DME with the sulfided $Ca/Pd/SiO_2$ mixed with γ-$Al_2O_3$ is then compared with that with the $Cu/ZnO/Al_2O_3$ catalyst mixed with γ-$Al_2O_3$. In the absence of $H_2S$ the sulfided $Ca/Pd/SiO_2$ with γ-$Al_2O_3$ yields 500 g methanol equiv. $kg_{cat}^{-1}$ $h^{-1}$ of DME at 613 K, 5.1 MPa and 20 $m^3$ (STP) $kg_{cat}^{-1}$ $h^{-1}$ (Fig. 22). On the other hand the STY of DME with the $Cu/ZnO/Al_2O_3$ catalyst with γ-$Al_2O_3$ is 1400 g methanol equiv. $kg_{cat}^{-1}$ $h^{-1}$ at 523 K, 5.1 MPa and 6 $m^3$ (STP) $kg_{cat}^{-1}$ $h^{-1}$, which is about three times higher than that with the sulfide sample with γ-$Al_2O_3$.

After reaching each steady-state activity under the sulfur-free conditions, the syngas containing $H_2S$ (100 ppm in concentration) was fed to the reactor. The DME STYs as a function of the total amount of $H_2S$ fed during the reactions are also shown in Fig. 22. Soon after the syngas containing $H_2S$ was fed into the reactor, the DME STY over the sulfided $Ca/Pd/SiO_2$ with γ-$Al_2O_3$ decreases to 70% of the initial value. Thereafter, this catalyst preserves a constant STY, i.e. 350 g methanol equiv. $kg_{cat}^{-1}$ $h^{-1}$ even when the total amount of $H_2S$ reaches 7.0 mol $H_2S$ mol $Pd^{-1}$. In contrast to the sulfide sample with γ-$Al_2O_3$ the DME STY over the $Cu/ZnO/Al_2O_3$ catalyst with γ-$Al_2O_3$ decreases quickly with increasing the total amount of $H_2S$ and eventually drops into 0. Our results clearly indicate that the sulfided $Ca/Pd/SiO_2$ mixed with γ-$Al_2O_3$ show the stable activity for the in situ DME synthesis even in the presence of $H_2S$ whereas the conventional catalyst is completely deactivated in the presence of $H_2S$.

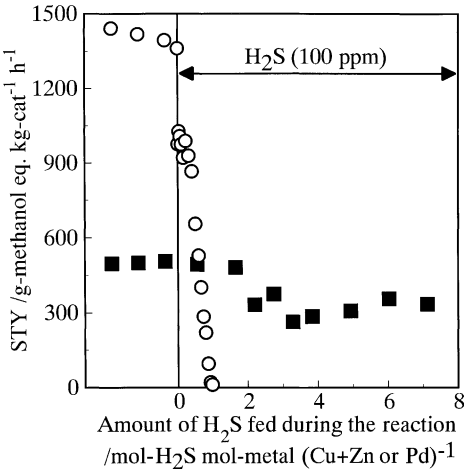


Fig. 22. Effect of $H_2S$ (100 ppm) on the activity for the synthesis of DME obtained with sulfided $Ca/Pd/SiO_2$ mixed with γ-$Al_2O_3$ (■), and commercial $Cu/ZnO/Al_2O_3$ catalyst mixed with γ-$Al_2O_3$ (○). Reaction conditions: 33% CO/62% $H_2$/5% Ar, 613 K, 5.1 MPa, 20 $m^3$ (STP) $kg_{cat}^{-1}$ $h^{-1}$ for sulfided $Ca/Pd/SiO_2$; 30% CO/60% $H_2$/5% $CO_2$/5% Ar, 523 K, 5.1 MPa, 6.0 $m^3$ (STP) $kg_{cat}^{-1}$ $h^{-1}$ for the $Cu/ZnO/Al_2O_3$ catalyst.

## 7. Conclusion

This review introduced the recent attempts to develop the sulfur tolerant catalysts for the FTS, $C_{2+}$ alcohol, methanol and/or DME synthesis. In particular, the discovery of the novel metal sulfide catalysts such as the Pd sulfide and the Rh sulfide have greatly enhanced possibilities of the methanol or DME synthesis without the desulfurizer unit from the syngas produced by, for example, the non-catalytic partial oxidation of biomass and waste plastics. Thus it is expected to contribute for developing the novel on-site process that produces the transportation fuels in the vicinity of small-scale and dispersed carbon resources.

The discovery of the novel metal sulfide catalysts is also expected to have a strong impact of the fields of the catalytic chemistry and the material science since we found the novel

catalysis of the transition metal sulfides. Further studies on the fine structure and the nature of the active site under the reaction conditions will contribute to develop much more active and selective catalysts.

## Acknowledgements

This work was partially supported by Research for the Future Program of Japan Society for the Promotion of Science under the Project "Synthesis of Ecological High Quality Transportation Fuels" (JSPS-RFTF98P01001). This work was also supported by the Ministry of Education, Culture, Sports, Science and Technology, a Grant-in-Aid for the 21st Century COE project, Giant Molecules and Complex Systems.

## References

[1] F. Fischer, Brennstoff-Chem. 16 (1935) 1–11.
[2] B.J. Wood, W.E. Isakson, H. Wise, Ind. Eng. Chem. Prod. Res. Dev. 19 (1980) 197–204.
[3] M. Berg, J. Koningen, K. Sjostrom, L. Waldheim, in: Development in Thermochemical Biomass Conversion, Blackie Academic & Professional, 1997, p. 1117.
[4] F.C. Jahnek, PETROTECH 22 (1999) 943–949.
[5] L. Xu, S. Bao, R.J. O'Brien, A. Raje, B.H. Davis, CHEMTECH 28 (1998) 47–53.
[6] J.F. Shultz, L.J.E. Hofer, F.S. Karn, R.B. Anderson, J. Phys. Chem. 66 (1962) 501–506.
[7] F.S. Karn, J.F. Shultz, R.E. Kelly, R.B. Anderson, Ind. Eng. Chem. Prod. Res. Dev. 2 (1963) 43–47.
[8] F.S. Karn, J.F. Shultz, R.E. Kelly, R.B. Anderson, Ind. Eng. Chem. Prod. Res. Dev. 3 (1964) 33–38.
[9] R.B. Anderson, F.S. Karn, J.F. Shultz, J. Catal. 4 (1965) 56–63.
[10] A.L. Chaffee, I. Campbell, N. Valentine, Appl. Catal. 47 (1989) 253–276.
[11] J. Barrault, C. Renard, Appl. Catal. 14 (1985) 133–143.
[12] G.J. Hutchings, J.C.A. Boeyens, J. Catal. 100 (1986) 507–511.
[13] G.J. Quarderer, K.A. Cochran, European Paten 0119609B1 (1991).
[14] C.B. Murchison, M.M. Conway, R.R. Stevens, G.J. Quarderer, in: Proceedings of the Ninth International Congress on Catalysis, vol. 2, 1988, pp. 626–632.
[15] J.W. Niemantsverdriet, A.M. van der Kraan, W.L. van Dijk, H.S. van der Baan, J. Phys. Chem. 84 (1980) 3363–3370.
[16] H. Jung, W.J. Thomson, J. Catal. 134 (1992) 654–667.
[17] D.B. Bukur, L. Nowicki, R.K. Manne, X. Lang, J. Catal. 155 (1995) 366–375.
[18] R.J. O'Brien, L. Xu, R.L. Spicer, B.H. Davis, Energy and Fuels 10 (1996) 921–926.
[19] G. Bian, A. Oonuki, Y. Kobayashi, N. Koizumi, M. Yamada, Appl. Catal. A: Gen. 219 (2001) 13–24.
[20] G. Bian, A. Oonuki, N. Koizumi, H. Nomoto, M. Yamada, J. Mol. Catal. 186 (2002) 203–213.
[21] A.P. Rale, B.H. Davis, Catal. Today 36 (1997) 335–345.
[22] R.J. O'Brien, L. Xu, R.L. Spicer, S. Bao, D.R. Milburn, B.H. Davis, Catal. Today 36 (1997) 325–334.
[23] B.H. Davis, Catal. Today 84 (2003) 83–98.
[24] H.W. Pennline, M.F. Zarochak, J.M. Stencel, R. Diehl, Ind. Eng. Chem. Res. 26 (1987) 595–601.
[25] N. Koizumi, Y. Kobayashi, M. Jiang, M. Yamada, Prepr. Am. Chem. Soc., Div. Petro. Chem. 45 (2000) 272–274.
[26] M. Jiang, N. Koizumi, M. Yamada, J. Phys. Chem. B 104 (2000) 7636–7643.
[27] U. Seip, I.C. Bassignana, J. Kuppers, G. Ertle, Surf. Sci. 160 (1985) 400–418.
[28] U. Seip, M.C. Tai, K. Christmann, J. Kuppers, G. Ertle, Surf. Sci. 139 (1984) 29–42.
[29] C.E. Bartosch, L.J. Whitman, W. Ho, J. Chem. Phys. 85 (1986) 1052–1060.
[30] J. Paul, Surf. Sci. 224 (1989) 348–358.
[31] P.B. Merrill, R.J. Madix, Surf. Sci. 271 (1992) 81–84.
[32] K.M. Rao, G. Spoto, E. Guglielminotti, A. Zecchina, Inorg. Chem. 28 (1989) 243–247.
[33] M. Jiang, N. Koizumi, T. Ozaki, M. Yamada, Appl. Catal. A: Gen. 209 (2001) 59–70.
[34] J.G. Santiesteban, C.E. Bogdan, R.G. Herman, K. Klier, in: Proceedings of the Ninth International Congress on Catalysis, vol. 2, 1988, pp. 561–568.
[35] P. Forzatti, E. Tronconi, I. Pasquon, Catal. Rev.-Sci. Eng. 33 (1991) 109–168.
[36] J.S. Lee, S. Kim, K.H. Lee, I.-S. Nam, J.S. Chung, Y.G. Kim, H.C. Woo, Appl. Catal. A: Gen. 110 (1994) 11–25.
[37] Y. Yoneyama, C. Song, Catal. Today 50 (1999) 19–27.
[38] T.A. Pecoraro, R.R. Chianelli, J. Catal. 67 (1981) 430–445.
[39] M. Yamada, N. Koizumi, A. Miyazawa, T. Furukawa, Catal. Lett. 78 (2002) 195–199.
[40] N. Koizumi, A. Miyazawa, T. Furukawa, M. Yamada, Chem. Lett. (2001) 1282–1283.
[41] S. Geller, Acta Cryst. 15 (1962) 1198–1201.
[42] J. Beck, T. Hilbert, Z. Anorg. Chem. 626 (2000) 72–79.
[43] E. Parthe, D. Hohnke, F. Hulliger, Acta Cryst. 23 (1967) 832–840.
[44] M. Ichikawa, Bull. Chem. Soc. Jpn. 51 (1978) 2268–2272.
[45] M. Ichikawa, K. Sekizawa, K. Shikakura, J. Mol. Catal. 11 (1981) 167–179.
[46] T.P. Wilson, P.H. Kasai, P.C. Ellgen, J. Catal. 69 (1981) 193–201.
[47] M.M. Bhasin, W.J. Bartley, P.C. Ellgen, T.P. Wilson, J. Catal. 54 (1978) 120–128.
[48] M. Kawai, M. Uda, M. Ichikawa, J. Phys. Chem. 89 (1985) 1654–1656.
[49] G.V.D. Lee, B. Schuller, H. Post, T.L.F. Favre, V. Ponec, J. Catal. 98 (1986) 522–529.
[50] G.V.D. Lee, V. Ponec, Catal. Rev.-Sci. Eng. 29 (2/3) (1987) 183–218.
[51] S.S.C. Chuang, S.I. Pien, J. Catal. 135 (1992) 618–634.
[52] S.S.C. Chuang, Appl. Catal. 66 (1990) L1–L6.
[53] N. Koizumi, K. Murai, S. Takasaki, M. Yamada, Prepr. Am. Chem. Soc., Div. Fuel Chem. 46 (2) (2001) 437–438.
[54] M.L. Poutsma, L.F. Elek, P.A. Ibarbia, A.P. Risch, J.A. Rabo, J. Catal. 52 (1978) 157–168.
[55] M. Ichikawa, K. Shikakura, Shokubai 21 (1979) 253–255.
[56] Y. Matsumura, W.-J. Shen, Y. Ichihashi, M. Okumura, J. Catal. 197 (2001) 267–272.
[57] N. Koizumi, K. Murai, S. Tamayama, T. Ozaki, M. Yamada, Energy and Fuels 17 (2003) 829–835.
[58] A. Gotti, R. Prins, J. Catal. 175 (1998) 302–311.
[59] Y. Kikuzono, S. Kagami, S. Naito, T. Onishi, K. Tamaru, Faraday Discuss. Chem. Soc. 72 (1981) 135–143.
[60] J.M. Driessen, E.K. Poels, J.P. Hindermann, V. Ponec, J. Catal. 82 (1983) 26–34.
[61] J.A. Anderson, M. López-Granados, M. Fernández-García, J. Catal. 176 (1998) 235–245.
[62] P.G. Gopal, R.L. Schneider, K.L. Watters, J. Catal. 105 (1987) 366–372.
[63] G.C. Cabilla, A.L. Bonivardi, M.A. Baltanás, J. Catal. 201 (2001) 213–220.
[64] Y. Zhang, Q. Sun, J. Deng, D. Wu, S. Chen, Appl. Catal. A: Gen. 158 (1997) 105–120.